Optimization of Passive Voltage Multipliers for Fast Start-up and Multi-voltage Power Supplies in Electromagnetic Energy Harvesting Systems

G Yang, B H Stark, S G Burrow and S J Hollis

University of Bristol, Bristol BS8 1TR, UK

E-mail: guang.yang@bristol.ac.uk

Abstract. This paper demonstrates the use of passive voltage multipliers for rapid start-up of sub-milliwatt electromagnetic energy harvesting systems. The work describes circuit optimization to make as short as possible the transition from completely depleted energy storage to the first powering-up of an actively controlled switched-mode converter. The dependency of the start-up time on component parameters and topologies is derived by simulation and experimentation. The resulting optimized multiplier design reduces the start-up time from several minutes to 1 second. An additional improvement uses the inherent cascade structure of the voltage multiplier to power sub-systems at different voltages. This multi-rail start-up is shown to reduce the circuit losses of the active converter by 72% with respect to the optimized single-rail system. The experimental results provide insight into the multiplier's transient behaviour, including circuit interactions, in a complete harvesting system, and offer important information to optimize voltage multipliers for rapid start-up.

1. Introduction

A significant challenge for an energy harvesting (EH) system with an active switched-mode converter between the harvester and main storage element is cold start [1], i.e., start-up with no previously stored energy. The most common cold-start solution is to use a parallel passive converter, e.g., a voltage multiplier, to charge the storage capacitor to the point where the converter's control circuits can be activated and supplied from this capacitor [2], as illustrated by the dashed arrows in Figure 1. This period of sub-optimum operation can take several minutes or even longer for sub-milliwatt harvesting, especially if the harvester is excited intermittently as is the case in many real environments [3].

This work presents a considerably faster start-up scheme: rather than charging the milifarad main storage capacitor to the required V_{store}, the start-up voltage multiplier output V_{cap} powers up the control of the active converter directly, as indicated by the bold arrow in Figure 1. The multiplier is optimized for rapid start-up, only having capacitances of microfarads as required to power the microwatt control circuits. Once the main converter has charged up the main energy storage, this becomes the supply for the converter's control circuits, thereby improving robustness.

For electromagnetic energy harvesting, voltage multipliers have been described in the literature for the main power extraction circuits [1], and optimized design described under specific load conditions. Typically the optimization includes minimizing the multiplier's output impedance at the harvester excitation frequency [4] and holding the output voltage constant at a value where the harvester is operating close to its maximum power point. By contrast, this paper investigates optimum multiplier design with rising output voltages, and the principal purpose is to make the charging time to reach a

pre-defined supply voltage as short as possible. The multiplier is thus open-circuited at the output during this period. We demonstrate further improvements by using the inherent cascade architecture (Figure 2a) of a voltage multiplier to supply several rails at different voltages.

The electromagnetic harvester used in this work produces a nominal 110 μW into a matched (360 Ω) load under a sinusoidal excitation of 1.5 $m \cdot s^{-2}$, at its resonant frequency of 44 Hz. Its full details have previously been published and can be found in [5].

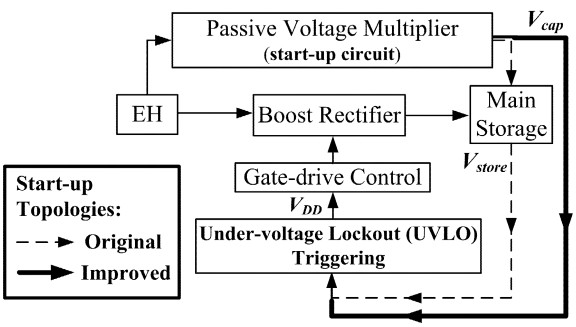

Figure 1. Improved start-up of active control of power conditioning subsystems.

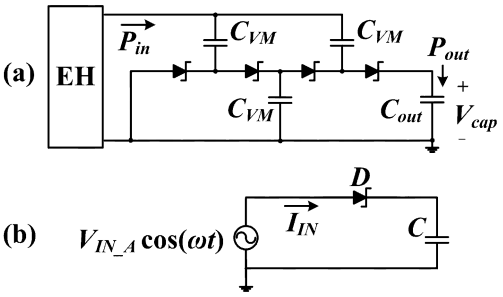

Figure 2. (a) Typical voltage multiplier, and (b) a single stage rectifier as its basic building block.

2. Analysis and optimization of voltage multipliers for fast start-up

2.1. Analysis of start-up time

For a given stored energy E_{store}, the start-up time t_{start} of a voltage multiplier (Figure 2a) is

$$E_{store} = \frac{1}{2} C_{out} V_{DD}^{\,2} = \int_0^{t_{start}} \left[P_{in}(t) - P_{out}(t) \right] \mathrm{d}t \quad , \tag{1}$$

where C_{out} is the multiplier output capacitance and V_{DD} is the required start-up voltage; the difference between the input power P_{in} and loss P_{loss} represents the charging power (i.e., P_{out} in Figure 2a). While P_{loss} is associated with the multiplier's constituent devices, e.g., the diode voltage drop and number of diodes, P_{in} is determined by the harvester loading condition, which varies continuously during start-up.

Here we present a simplified analysis of the dynamic loading by considering a single-stage rectifier as the basic building block, Figure 2b. The rectifier draws current $i_{IN}(t)$ from a sinusoidal input voltage source $v_{IN}(t) = V_{IN\_A} \cdot \cos \omega t$. Thus, the diode current (exponential) is $i_D = I_S \cdot \exp(v_D / n\phi_t - 1)$, where I_S is the diode saturation current, ϕ_t is the thermal voltage, and n is the slope factor. The diode's voltage drop is $v_D(t) = V_{IN\_A} \cdot \cos \omega t - V_{cap}(t)$, and the resistance emulated by the rectifier is governed by

$$r_e(t) = \frac{v_{IN}(t)}{i_{IN}(t)} = \frac{V_{IN\_A} \cos \omega t}{I_S \cdot [\exp(V_{IN\_A} \cos \omega t - V_{cap}(t)) / n\phi_t - 1]} \quad . \tag{2}$$

It follows that the resistance $r_e(t)$ varies not only within every input cycle but also as the capacitor is charged during start-up and $V_{cap}(t)$ increases. This relationship becomes more complicated when the input source in Figure 2b is replaced by the actual harvester-generated voltage, since this voltage is now dependent on the loading represented by $r_e(t)$ and with time-varying amplitude. The slower the rate of change of the dynamic loading condition, the closer this condition approximates the optimum steady-state loading condition of the harvester, as demonstrated in [5]. This suggests the use of large multiplier capacitances (C_{VM} in Figure 2a) to maximise the input power, because the larger the capacitance, the more slowly $V_{cap}(t)$ increases during start-up, and thus the more slowly $r_e(t)$ increases in equation (2). Larger capacitances, however, result in longer changing time for each multiplier-stage. A good trade-off is thus required here to minimize start-up time.

2.2. Component selection to minimize start-up time

Start-up of the gate-drive control (Figure 1) occurs at 0.9 V corresponding to the minimum operating voltage of a TS3001 low-power pulse-width-modulation (PWM) generator used here. As suggested by equation (1), the lower the required rail, the shorter the start-up time. A multiplier-output capacitance

of C_{out} = 47 µF is used through the optimization, as this storage is suitable for microwatt loads. The default magnitude of the harvester's excitation is 1.5 m·s^{-2} corresponding to a maximum harvestable power P_{max} = 110 µW. During low-voltage start-up, the diode's forward-voltage drop is the primary source of power loss. This points towards the use of low-threshold diodes, but typically the lower the threshold is, the higher the leakage is. Four different Schottky diodes are thus evaluated through PSpice simulation: RB411D, BAT760, BAT754, and 1PS79SB30. Despite the RB411D diode having the highest leakage (2.5 µA @ 1 V), the benefit of its low voltage drop of ~90 mV for 100-µA forward current outweighs the drawback of high leakage and results in the fastest start-up. It is thus selected.

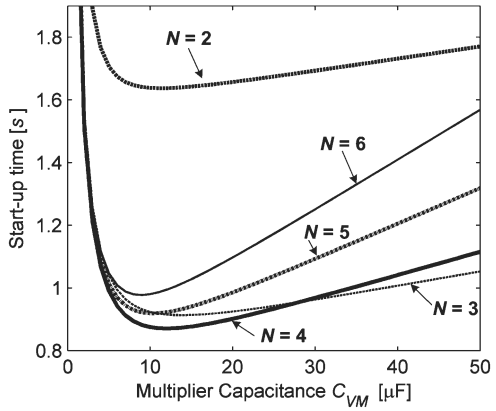

Figure 3. Simulated start-up times for V_{cap} = 0.9 V versus multiplier capacitance C_{VM}, for different stage numbers N.

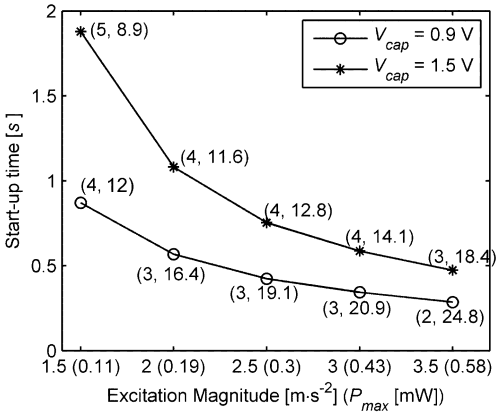

Figure 4. Simulated start-up times of optimized combinations of N and C_{VM} for V_{cap} = 0.9 V and 1.5 V, against harvester excitation.

Figure 3 shows the start-up time as the multiplier capacitance C_{VM} and the number of multiplier stages N are varied. The shortest time is found using N = 4 and C_{VM} = 12 µF. Larger capacitances slow down the start-up, but too small ones, which cause undesired harvester-loading, also increase the time sharply. A sufficient stage number is required for voltage boosting and offers faster start-up, whilst too many stages increase the total power losses, resulting in inefficient start-up. As the total stage number increases, varying each stage capacitance has increased effects on the total power losses and harvester loading, which in turn results in higher dependence of the start-up time on the capacitance, as seen by the increasing gradients in Figure 3. Figure 4 shows the implication of requiring a higher start-up voltage of 1.5 V. The start-up time increases, especially at low excitation magnitudes and hence low maximum harvestable power P_{max}. As the excitation increases, the start-up time shortens, with larger optimal C_{VM} and smaller optimal N. This is due to their impact on the harvester loading and utilisation.

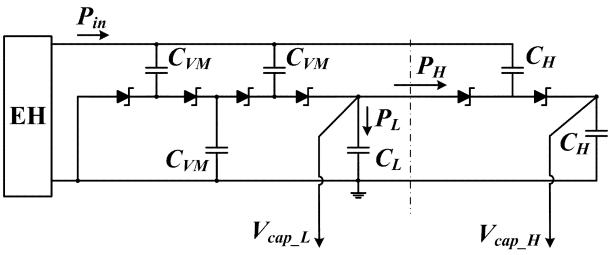

Figure 5. Dual-rail ($V_{cap\_L,\,H}$) start-up topology of a voltage multiplier.

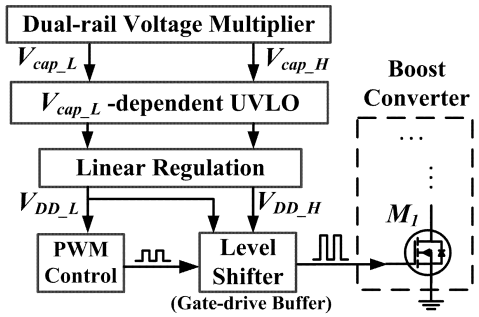

Figure 6. Prototyped dual-rail power supply for PWM control of a boost converter.

2.3. Multi-rail start-up

The single-rail start-up system suffers from a trade-off, where choosing a lower rail voltage shortens the start-up time but also increases the circuit loss of the main converter due to insufficient headroom above the gate threshold voltage. This trade-off can be improved through the powering up of different subsystems with different voltage rails. Fortunately, the voltage multiplier readily provides different

internal voltages, see Figure 5, where, during start-up, the rails V_{cap_L} and V_{cap_H} rise simultaneously with $V_{cap\_H} > V_{cap\_L}$. The resulting system is illustrated in Figure 6. The majority of the control circuits are powered by the lower rail V_{DD_L}, which reduces the total quiescent power consumption, and permits these circuits to be triggered sooner via an under-voltage-lockout (UVLO). The higher rail V_{DD_H} powers only the gate-drive buffer to provide sufficient headroom above the gate threshold voltage of the main switching device M_1, thereby achieving low on-state resistance and conduction loss. Improved trade-offs between start-up speed, quiescent power overheads of active control, and power-conversion efficiency can thus be expected. In the circuit of Figure 5, the choice of C_H affects the start-up speed of V_{cap_L}, because the larger capacitance C_H is, the more power P_H is drawn from stage $N = 4$, and therefore less power P_L is available to charge C_L. Using a small C_H improves the start-up speed while the actual required C_H is small as it is only used to power the gate-drive buffer.

3. Experimental results

3.1. Measurements of transient power during start-up of single-rail system

As suggested in equation (1), the start-up time is determined by the varying input power and power loss. The input and output transient power (averaged over every excitation cycle) of the voltage multiplier of Figure 2a is measured during a start-up event and plotted in Figures 7, 8 and 9, as a function of C_{VM}, showing that these powers vary dynamically. Figure 7 shows that larger capacitances C_{VM} improve the harvester loading, as seen by the higher input powers, but also increase the power loss, which results in an optimal C_{VM} at 12 µF yielding the highest output power.

Figure 8 shows that the output powers peak at different output voltages for different stage numbers N. A higher N shifts the power peak to the higher voltage, as it provides higher voltage-boosting. This also improves the harvester loading, as each multiplier-stage draws power from its preceding stage so that charging the first stage takes more time. The resulting loading changes slowly and approaches the optimum steady-state loading condition, as noted in Section 2.1. Higher N with more diodes, however, results in higher loss. Thus, the optimal N is 4, whose corresponding output power peaks at the rail 0.9 V. With C_{VM} =12 µF, it offers the shortest start-up time for P_{max} = 110 µW as shown in Figure 3.

Figure 9 shows that different excitation magnitudes (whilst $N = 4$, C_{VM} =12 µF) not only change the power peaks but also their voltage locations. Since higher excitations and hence input power levels P_{max} result in higher voltages at which the powers peak, lower N is required to shift the peak from a low voltage level to the targeted rail, in order to achieve the fastest start-up, as shown in Figure 4.

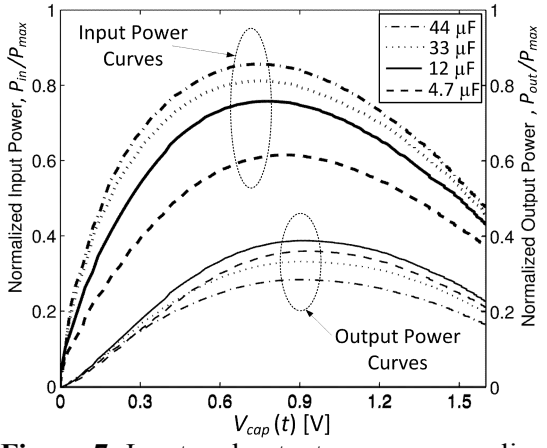

Figure 7. Input and output powers normalized to the maximum harvestable power P_{max}, and measured as the output voltage V_{cap} increases during start-up, for different C_{VM} values.

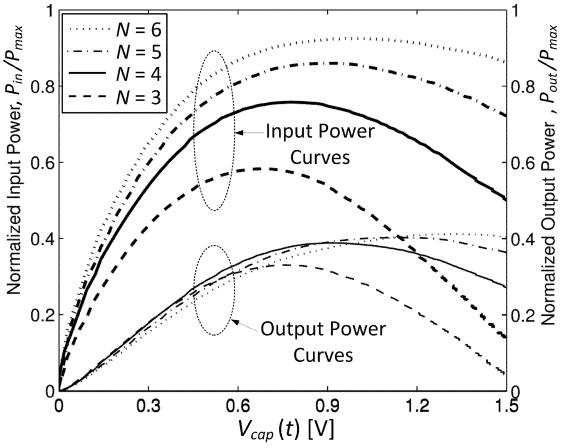

Figure 8. Normalized input and output powers, measured as the output voltage increases during start-up, for different stage numbers N.

3.2. Measurements of the dual-rail system

The dual-rail system of Figure 6 is prototyped using discrete devices including the TS12001 UVLO detector, the TS3001 PWM generator, and the NLSV1T34 level shifter (circuit details can be found in

[2] and [3]). The system is compared with its single-rail counterpart using the circuit shown in Figure 2a with $V_{DD} = V_{cap}$. Figure 10 shows the steady-state measurement results. The higher the single-rail V_{DD} is, the higher the quiescent power consumption P_q is, and the lower the converter's conduction loss P_{cond} is, since the rail regulates the gate-drive signal swing. This results in an optimal V_{DD} at 1.2 V corresponding to the lowest total power loss P_{loss}. By contrast, even lower P_{loss} is achieved by the dual-rail system with V_{DD_L} at 0.9 V for low P_q and V_{DD_H} at 1.5 V for low P_{cond}. These results, together with the measured start-up times, are summarized in Table 1. The single-rail 0.9 V start-up offers the shortest time but results in much higher P_{loss}. An improved trade-off is achieved here by the dual-rail system using small capacitances C_H in Figure 5; the total power loss is reduced by about 72%, whilst the optimized start-up time is ~1 s, as opposed to the 148 s presented in [2], under similar conditions.

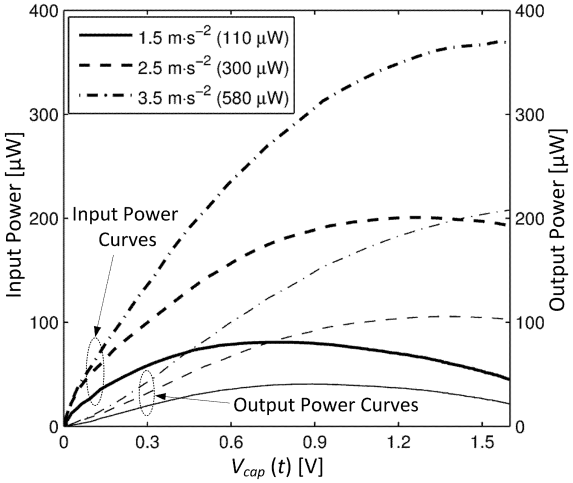

Figure 9. Input and output powers, measured as the output voltage increases during start-up, for different harvester-excitation magnitudes.

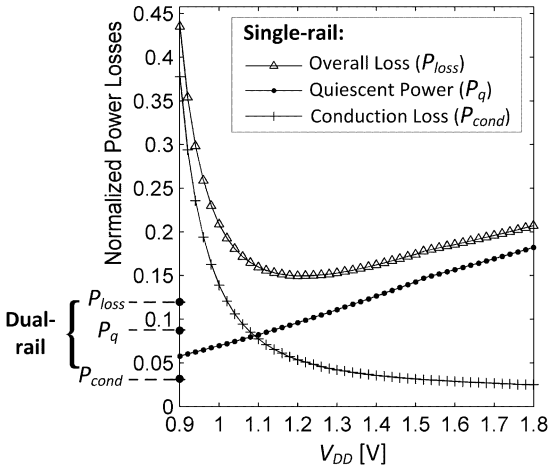

Figure 10. Steady-state measured power losses (normalized to P_{max}) of the single-rail system against the start-up rail V_{DD}, and of the dual-rail system with V_{DD_L} = 0.9 V and V_{DD_H} = 1.5 V.

Table 1. Comparative summary of the single-rail and dual-rail power-supply systems.

Power Supplies	Power Losses (relative to max. harvestable power)			Start-up Time ($C_{out} = C_L$ = 47 µF) [s]
	Quiescent, P_q	Conduction, P_{cond}	Overall, P_{loss}	
Single-rail of V_{DD} = 0.9 V	5.8%	37.8%	43.6%	0.94 @C_{VM} = 12 µF (optimum)
Single-rail of V_{DD} = 1.2 V	9.6%	5.4%	15%	1.39 @C_{VM} = 10 µF (optimum)
Dual-rail of V_{DD_L} = 0.9 V V_{DD_H} = 1.5 V	8.8%	3.2%	12%	1.03 @C_H = 2.2 µF, C_{VM} = 12 µF 1.13 @C_H = 4.7 µF, C_{VM} = 12 µF 1.2 @C_H = 6.8 µF, C_{VM} = 12 µF

4. Conclusion

For microwatt electromagnetic harvesting systems, start-up using passive voltage multipliers can be shortened by selecting stage numbers and capacitances to achieve peak output power at the targeted rail voltage for given input power levels. Furthermore, by using the proposed multi-rail multiplier topology which distributes supply rails to various subsystems, an improved trade-off between start-up speed and active power conversion efficiency is found, resulting in a ~1 second start-up and a ~72% reduction in power loss with respect to the single-rail system.

References

[1] Torah R N, Tudor M J, Patel K, Garcia I N, and Beeby S P 2007 *Proc. IEEE Sensors (Atlanta)* p 264–7
[2] Szarka G D, Burrow S G, and Stark B H 2013 *IEEE Trans. Power Electron*. **28** 3353-62
[3] Yang G, Stark B H, Hollis S J, and Burrow S G 2014 *IEEE J. Emerg. Sel. Topics Circuits Syst*. **4** 364–74
[4] Lin P M 1977 *IEEE Trans. Circ. Syst*. **CAS-24** 517–30
[5] Szarka G D, Proynov P P, Stark B H, and Burrow S G 2014 *IEEE Trans. Power Electron*. **29** 201–12